

Full Length Research Paper

Calibrating the multiple orifice mathematical model using physical scale model foam at low Reynolds number

M. Emmanuel Adigio

Department of Mechanical Engineering, Niger Delta University, Wilberforce Island, Amassoma, Bayelsa State, Nigeria.
E-mail: emadigio@yahoo.com.

Accepted 27 July 2010

Recently, gelcast ceramic foams are being considered as potential diesel particulate filter substrates. Consequently, a mathematical model known as the Multiple Orifice Mathematical (MOM) model for the study of fluid flow and the determination of pressure gradients across the foam filters was developed and calibrated by some researchers. However, there was need to establish the model application on a wider range of pore sizes of the foam filters. Hence, this work is to establish the dynamic similarity of the physical scale model used for the calibration and the ceramic foams. Following the conceptual model employed in the development of the MOM model, generic physical scale foam models and a fluid flow rig was fabricated. The pressure drops across the generic physical model foam obtained from experiments over different ranges of low Reynolds number were graph-fitted against the MOM model to determine the kinetic correction factors. The values for the kinetic correction coefficient determined from the generic physical model at low Reynolds number is within the range obtained by other researchers in the calibration of the MOM model, which implies that the MOM model can be applied to a wide range of pore sizes found in gelcast ceramic foam filters.

Key words: Diesel particulate trap, gelcast ceramic foam, kinetic correction coefficient, generic foams, foam filters, pressure gradients.

INTRODUCTION

Engine manufacturers have made progress in the reduction of diesel engine emissions through improved engine design (Swiss Agency for the Environment, Forest and Landscape, 2000a; Mayer, 1998], fuel formulation and improved maintenance practices. Modern diesel engine is reported to have reduced particulate matter (PM) emission by as much as 90% (Mayer, 1998; Nauss, 1997) through the improved engine design and as much as 30% through fuel formulation. Mayer et al. (1998) reported that PM emissions from diesel engines fall in the size range of up to 100 nm and the new engines in particular emit more fine particulates at all operating conditions.

The consequence of improved engine design and fuel formulation is a decrease in PM mass but an increase in

fine particulate number which is potentially more hazardous (Mayer, 1998). The key factor for the determination of the effect of diesel particulates on health is their size. Particles that are < 100 nm are invisible to the eyes but can deposit in the bronchial and pulmonary tracts of the respiratory system (Hinds, 1980). It is reported by many researchers (Nikula et al., 1999; Health Effects Institute, 2002; United State Environmental Protection Agency, 2002; Dybdahl et al., 2003; World Health Organization, 2003; Garshick et al., 2004; Warheit et al., 2004; Brown et al., 2004; Arey, 2004) that diesel exhaust emissions affect health and contribute to acid rain and visibility. Siegmann and Siegmann (1997) reported that fine particles from combustion contain thousands of different chemicals that cannot be characterized due to their un-

stable condition in the atmosphere.

Consequently, there is expected to be a need for after treatment of the exhaust gases to meet future emission limits (Swiss Agency for the Environment, Forest and Landscape, 2000). The diesel particulate filter technology has been proven as a viable option for the effective reduction of PM from diesel engines (Swiss Agency for the Environment, Forest and Landscape, 2000b) and mathematical modelling is increasingly becoming an engineering tool to understand, predict and control the diesel particulate filter (DPF) systems. DPFs consist of a filter designed to collect the PM in the exhaust stream of the diesel engine, while allowing the exhaust gases to pass through the system. The fundamental parameters to assess the quality of the DPF are the filtration efficiency and the pressure drop of the filter. Hence, it is desirable to develop mathematical models to predict these parameters that can be used within given boundary conditions to aid the design of DPFs.

Ceramic foams until recently were mainly used as catalyst supports (Richardson et al., 2000) and molten metal filters (Gabathuler et al., 1991). However, they are now being considered for DPF applications since they exhibit some favorable attributes. Ceramic foams have good filtration in the nano-particle range (Pontikakis et al., 2001). The high porous nature of ceramic foam filters is favorable to the propagation of the combustion zone during regeneration.

The modelling of porous media such as the ceramic foam filters, however, has been of interest to significantly fewer researchers. A work, of interest, reported by Pontikakis et al. (2001) is the development of a mathematical model for the prediction of pressure drop across reticulated foam filters. Pontikakis et al. (2001) assumed that the struts which form the solid frame work of foam filters can be modeled as fiber elements. Other researchers (Adigio et al., 2008) reported the development of a mathematical model referred to as "Multiple Orifice Mathematical (MOM) model" for understanding fluid flow through the filters and an aid for filter design. This MOM model was developed by applying the fluid flow theory on a simplified conceptual model, where the ceramic foam was represented with rows of cells across the filter, connected by openings called the windows. The resultant mathematical model was calibrated by fixing the viscous correction coefficient to determine the kinetic correction coefficient, β by "graph fitting" the mathematical model on a graph developed from experimental data of fluid flow on a generic physical scale model foam filter.

This report presents the calibration of the MOM model using experimental data from generic physical scale model foam of external diameter 60 mm and lengths of 100 and 125 mm at low flow rate, thus, Reynolds number ranging from 35 to 890. This was necessary because it was observed that the flow rates through the ceramic foam filters samples are low and the corresponding Reynolds number is within the above range. The aim of

this study is to establish the dynamic similarity of the physical scale model foam and the ceramic foam filter samples used for the model validation, thus, confirming the general application of the MOM model on gelcast ceramic foam filters.

MATERIALS AND METHODS

The generic physical scale model foam samples used for the model calibration are based on a combination of five pieces of foams of length 25 mm and diameter 60 mm, which are reproduction of the conceptual model used for the development of the MOM model, where the cells are arrayed across the length of the foam with connecting windows. The method used in the manufacture of the model foam is a rapid manufacturing process known as stereolithography (SL). The rapid manufacturing refers to a class of technologies that can automatically produce physical models from computer assisted design (CAD) data. The structure is illustrated by a Solid Edge (Version 15) as shown in Figure 1.

The advantage of using the SL method to produce the generic physical scale model foam lies in the accuracy of the process and the ability to produce complex geometries without the need to resort to mould tooling, therefore, the relatively complex structure of the filter could be manufactured comparatively easily. This would have been difficult to achieve with other manufacturing approaches, or indeed on a real ceramic foam sample.

An experimental rig was designed using the Solid Edge CAD Package and constructed to measure the pressure drop across the model foam filter samples, the flow rates through them, and the temperature of the fluid is shown in Figure 2. A flow conditioner was mounted on the rig to straighten the swirling air flow and reduce the pulsating effect from the centrifugal blower that generates the air flow. The distance from the conditioner to the orifice plate was more than ten times the pipe diameter to allow the full development of the fluid flow before the orifice plate. Flow rates were measured using a calibrated orifice flow meter designed and assembled in accordance to the ISO 5167 standard (BS EN ISO 5167, 2003). Using the Reader-Harris/Gallagher Equation (Reader-Harris and McNaught, 2005) the values of the orifice discharge coefficients (C_d) corresponding to the 15 mm orifice diameter plate was calculated to be 0.6285. The absolute pressure and temperature were measured before the filter holder to determine the density of the air flowing through the rig. The experiments on the model foam samples were repeated three times to assure repeatability of the results obtained.

The data was collected from filters of lengths 100 and 125 mm which are made up of 25 mm \times 4 pieces and 25 mm \times 5 pieces of generic physical model foam samples respectively. The samples have cell size of 7.0 mm and porosity of 80%. The data was collected at three ranges of Reynolds number by adjusting the flow rates across the filters accordingly; 148 to 890, 86 to 269 and 35 to 99 respectively, and graphs corresponding to each range were produced.

RESULTS

Figures 3, 4 and 5 show the MOM model calibration graphs of pressure gradients vs. fluid mass flow rate developed from the experimental data presented in Tables 1, 2 and 3 respectively. The graphs demonstrate the graph-fitting of the model where the value of the kinetic correction coefficient β in the MOM model (Equation 3) was adjusted until the model fits the graphs

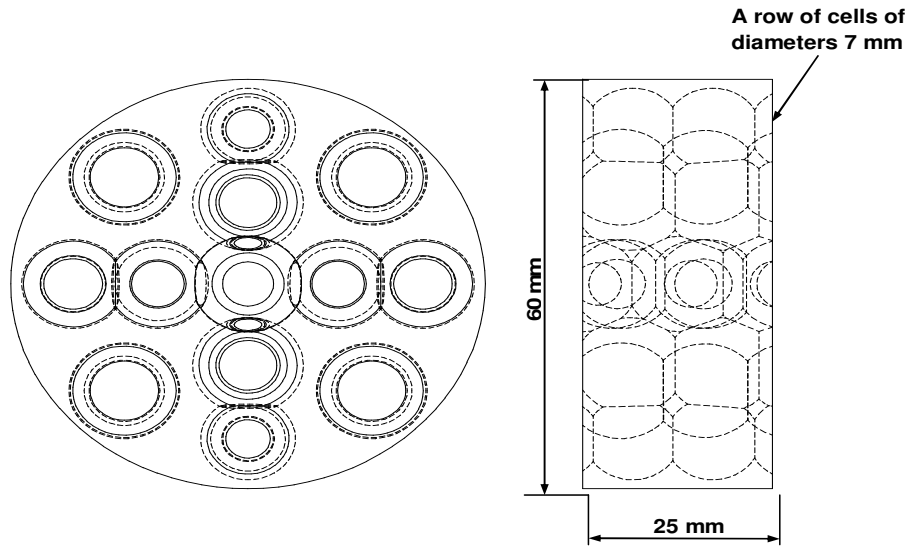


Figure 1. A generic multiple orifice physical scale model designed using a CAD package.

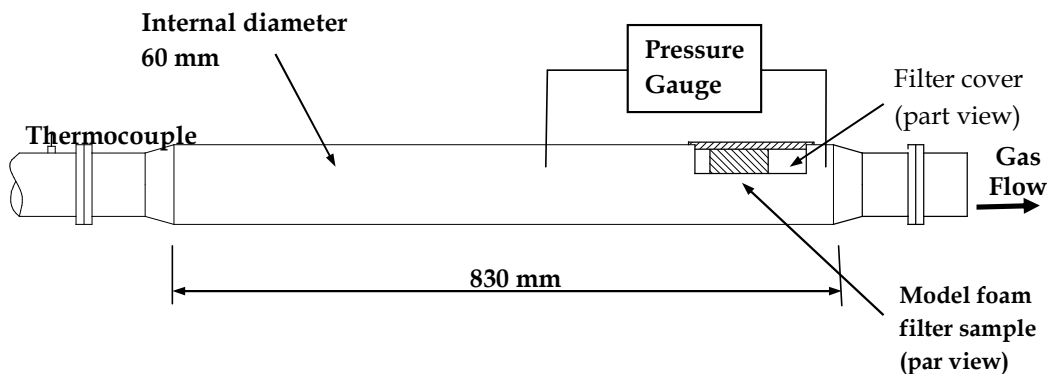


Figure 2. Schematic diagram of a flow rig model foam sample holder.

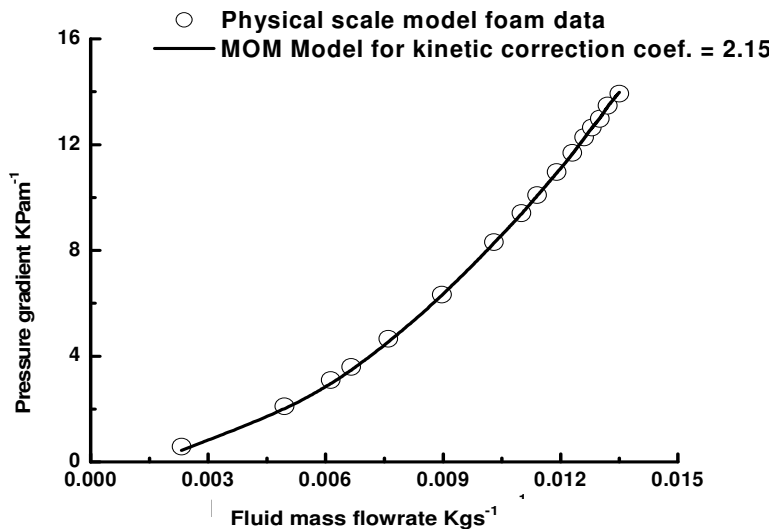


Figure 3. Graph of pressure gradient vs. fluid flow rate in a physical scale model foam sample, for the calibration of the MOM model. Reynolds number is from 148 to 890.

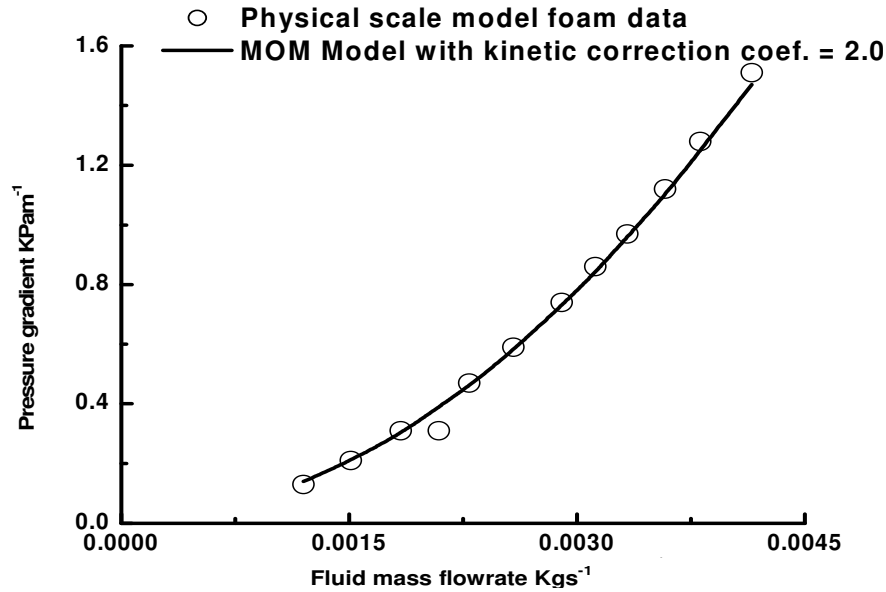


Figure 4. Graph of pressure gradient vs. fluid flow rate in a physical scale model foam sample, for the calibration of the MOM model. Reynolds number is from 86 to 269.

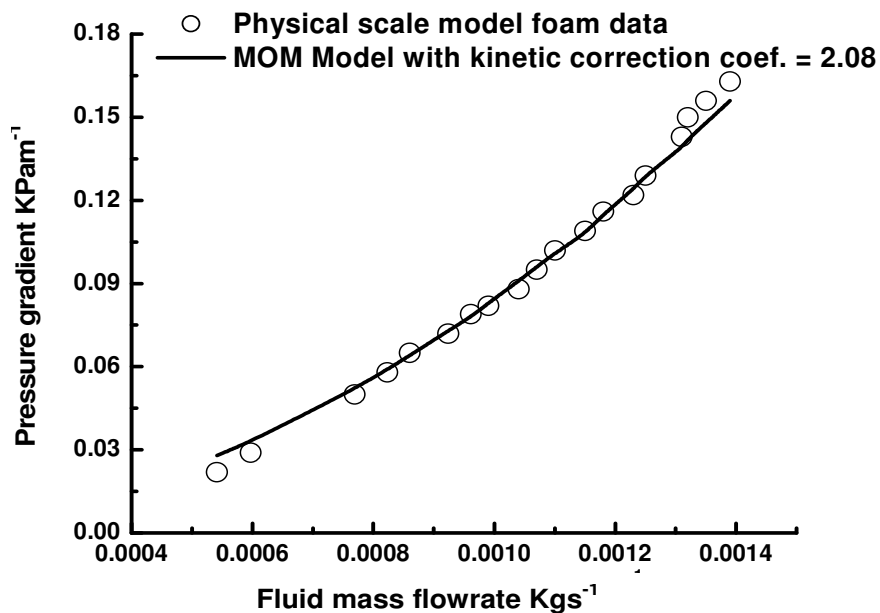


Figure 5. Graph of pressure gradient vs. fluid flow rate in a physical scale model foam sample, for the calibration of the MOM model. Reynolds number is from 35 to 99.

developed from the experimental data. The corresponding kinetic correction coefficients are indicated on the graphs.

DISCUSSIONS

In computing the experimental data to calculate the mass flow rate of the fluid, the densities were determined from

the ideal gas law, $\rho = p / RT$, where R is the universal gas constant equal to $287 \text{ Jkg}^{-1}\text{K}^{-1}$, T is the absolute temperature in Kelvin, K, and p is the gas pressure in Pascal, Pa. The mass flow rate is the product of the volumetric flow rate, Q (m^3s^{-1}) and the fluid density, that is,

$$\text{Mass flow rate} = \rho Q \tag{1}$$

Consequently, the fluid mass flow rate is determined by

Table 1. Physical scale model foam of length 100 mm, cell diameter = 7.0 mm and porosity = 80%, Reynolds number is from 148 to 890.

| P_{orif} (Pa) | P_{filt} (Pa) | T (°C) | P_{abs} (Pa) | Air mass flow rate (kgs ⁻¹) | Pgrad. (kPam ⁻¹) | Pgcal. (kPam ⁻¹) |
|------------------------|------------------------|--------|-----------------------|---|------------------------------|------------------------------|
| 21 | 59 | 26.9 | 56 | 2.32E-03 | 0.59 | 0.44 |
| 96 | 211 | 27.3 | 200 | 4.95E-03 | 2.11 | 1.94 |
| 147 | 310 | 27.6 | 290 | 6.13E-03 | 3.10 | 2.95 |
| 173 | 360 | 28 | 338 | 6.65E-03 | 3.60 | 3.46 |
| 226 | 466 | 28.2 | 436 | 7.60E-03 | 4.66 | 4.51 |
| 315 | 634 | 28.8 | 594 | 8.97E-03 | 6.34 | 6.26 |
| 417 | 832 | 29 | 779 | 1.03E-02 | 8.32 | 8.27 |
| 473 | 941 | 29.5 | 884 | 1.10E-02 | 9.41 | 9.37 |
| 509 | 1010 | 29.6 | 948 | 1.14E-02 | 10.10 | 10.07 |
| 552 | 1097 | 29.8 | 1029 | 1.19E-02 | 10.97 | 10.92 |
| 589 | 1169 | 29.9 | 1097 | 1.23E-02 | 11.69 | 11.64 |
| 619 | 1228 | 29.9 | 1152 | 1.26E-02 | 12.28 | 12.23 |
| 640 | 1265 | 30 | 1190 | 1.28E-02 | 12.65 | 12.64 |
| 657 | 1298 | 30 | 1220 | 1.30E-02 | 12.98 | 12.98 |
| 681 | 1348 | 30 | 1266 | 1.32E-02 | 13.48 | 13.45 |
| 708 | 1393 | 29.9 | 1310 | 1.35E-02 | 13.93 | 13.98 |

Table 2. Physical scale model foam of length 100 mm, cell diameter = 7.0 mm and porosity = 80%, Reynolds number is from 86 to 269.

| P_{orif} (Pa) | P_{filt} (Pa) | T (°C) | P_{abs} (Pa) | Air mass flow rate kg s ⁻¹ | Pgrad. kPa m ⁻¹ | Pgcal. kPa m ⁻¹ |
|------------------------|------------------------|--------|-----------------------|---------------------------------------|----------------------------|----------------------------|
| 50 | 13 | 20.7 | 15 | 1.20E-03 | 0.13 | 0.14 |
| 79 | 21 | 20.7 | 23 | 1.51E-03 | 0.21 | 0.21 |
| 118 | 31 | 20.7 | 33 | 1.84E-03 | 0.31 | 0.30 |
| 151 | 31 | 20.7 | 43 | 2.09E-03 | 0.31 | 0.39 |
| 181 | 47 | 20.7 | 51 | 2.29E-03 | 0.47 | 0.46 |
| 231 | 59 | 20.8 | 65 | 2.58E-03 | 0.59 | 0.58 |
| 292 | 74 | 20.9 | 81 | 2.90E-03 | 0.74 | 0.73 |
| 337 | 86 | 21 | 94 | 3.12E-03 | 0.86 | 0.84 |
| 384 | 97 | 21.1 | 107 | 3.33E-03 | 0.97 | 0.96 |
| 444 | 112 | 21.2 | 123 | 3.58E-03 | 1.12 | 1.10 |
| 504 | 128 | 21.3 | 139 | 3.81E-03 | 1.28 | 1.25 |
| 597 | 151 | 21.4 | 165 | 4.15E-03 | 1.51 | 1.47 |

developing a relationship between flow rate and pressure difference across the orifice plate, thus, applying the Bernoulli equation across the orifice plate then simplifying gives the following relationship,

$$\rho Q = C_D \frac{\pi}{4} D_o^2 \sqrt{\frac{2\rho\Delta p}{(1 - (\frac{D_o}{D_i})^4)}} \quad 2$$

where C_D is the orifice plate discharge coefficient, D_o is the orifice diameter, ρ is the fluid density, D_i is the pipe diameter and Δp is the pressure difference measured across the orifice plate.

The first four columns of Tables 1, 2 and 3 (pressure difference across orifice P_{orif} , pressure difference across

filter P_{filt} , temperature T and absolute pressure P_{abs}) were measurements from the experimental rig while the remaining columns were calculated from appropriate relationships. The atmospheric pressure was also measured during the experiments to enable the calculation of the air mass flow rate. The air mass flow rate was calculated from Equation 2. The pressure gradients across the filter from the experimental data were the ratio of the pressure difference across the filter and the filter length.

The last column is the calculated pressure gradients. Across the filters using the MOM model (Equation 3) (Adigio et al., 2008), by primarily adjusting the Kinetic correction coefficient β for a given foam window and cell size and filter length, until the model graph fits to the graphs developed from the experimental data.

Table 3. Physical scale model foam of length 125 mm, cell diameter = 7.0 mm and porosity = 80%, Reynolds number is from 35 to 99.

| P _{orif} (Pa) | P _{filt} (Pa) | T (°C) | P _{abs} (Pa) | Air mass flow rate (kgs ⁻¹) | P _{grad.} (kPm ⁻¹) | P _{gcal.} (kPam ⁻¹) |
|------------------------|------------------------|--------|-----------------------|---|---|--|
| 10 | 3 | 22.1 | 4 | 5.41E-04 | 0.022 | 0.028 |
| 12 | 4 | 22.1 | 6 | 5.97E-04 | 0.029 | 0.033 |
| 21 | 6 | 22.4 | 10 | 7.69E-04 | 0.050 | 0.052 |
| 24 | 7 | 22.4 | 12 | 8.23E-04 | 0.058 | 0.059 |
| 26 | 8 | 22.4 | 13 | 8.60E-04 | 0.065 | 0.064 |
| 30 | 9 | 22.5 | 14 | 9.24E-04 | 0.072 | 0.073 |
| 32 | 10 | 22.5 | 16 | 9.61E-04 | 0.079 | 0.078 |
| 34 | 10 | 22.6 | 17 | 9.90E-04 | 0.082 | 0.083 |
| 38 | 11 | 22.6 | 18 | 1.04E-03 | 0.088 | 0.091 |
| 40 | 12 | 22.7 | 19 | 1.07E-03 | 0.095 | 0.096 |
| 43 | 13 | 22.7 | 21 | 1.10E-03 | 0.102 | 0.101 |
| 46 | 14 | 22.8 | 22 | 1.15E-03 | 0.109 | 0.108 |
| 49 | 14 | 22.9 | 24 | 1.18E-03 | 0.116 | 0.115 |
| 53 | 15 | 23 | 25 | 1.23E-03 | 0.122 | 0.124 |
| 55 | 16 | 23.1 | 27 | 1.25E-03 | 0.129 | 0.129 |
| 60 | 18 | 23.1 | 29 | 1.31E-03 | 0.143 | 0.139 |
| 61 | 19 | 23.3 | 30 | 1.32E-03 | 0.150 | 0.142 |
| 64 | 20 | 23.5 | 31 | 1.35E-03 | 0.156 | 0.148 |
| 68 | 20 | 23.5 | 33 | 1.39E-03 | 0.163 | 0.156 |

$$\frac{\Delta p}{L} = \frac{\alpha \mu A (1-\epsilon)^2}{D^2 \pi \epsilon^3} S_v^2 Q + \frac{(1-w^4/d_o^4)}{\sqrt{d^2-w^2}} \left[\frac{d_o^2}{\beta \pi D^2 w^2} \right]^2 8 \rho Q^2$$

where $d_o = \left[\frac{d^3 (2 - 3B(3k^2 + B^2))}{3\sqrt{d^2 - w^2}} \right]^{0.5}$

$$B = 1 - \sqrt{1 - k^2} \text{ and } k = w/d$$

α is the viscous pressure loss correction coefficient which was chosen and fixed at 5 as suggested by MacDonald et al. (1979), w and d are the window and cell size respectively. The specific surface, S_v was calculated from the expression below developed by Adigio et al. (2008);

$$S_v = \frac{12[1 - 6B + 5k^2 / 2]\epsilon}{d[2 - 3B(3k^2 + B^2)][1 - \epsilon]}$$

The graphs (Figures 3, 4 and 5) shows that the kinetic correction coefficients obtained from the three ranges of Reynolds numbers varied from 2.0 to 2.15. These values of kinetic correction coefficients determined from the use of the multiple orifice physical scale model corroborates the results offered by Adigio et al. (2008).

Conclusion

A cost effective, accurate and rapid methodology was developed to evaluate the general use of the MOM model in the study of fluid flow through gelcast ceramic foam filters. The kinetic correction coefficient β of the MOM model has been determined by graph fitting the mathematical model to experimental data obtained from generic physical scale model foams. The corresponding values of kinetic correction coefficient are 2.15, 2.0 and 2.08 respectively, which lie within the range established by Adigio et al. (2008). This implies that the kinetic correction coefficient for the MOM model is independent of the Reynolds number. Hence, this research work has established the use of the MOM model as a potential tool in the study of fluid flow and diesel particulate filter design in a wide range of filter cell sizes found in gelcast ceramic foam filters.

The application of the mathematical model can be extended to other types of foams, including reticulated foams. The model can also be extended to the development of filtration efficiency modelling in foam filters which are also a tool in filter design and the understanding of fluid flow in porous materials.

ACKNOWLEDGEMENTS

The author acknowledges the Niger Delta University Bayelsa State, Nigeria for financial support. The author

also thanks Loughborough University, UK for technical support. Particular thanks must go to the author's research supervisor Colin Garner for his untiring encouragement and Head of Department, P. P. Jombo for his understanding.

REFERENCES

- Adigio EM, Binner JGP, Garner CP, Hague RJ, Williams AM (2008). Modeling gas flow pressure gradients in gelcast ceramic foam diesel particulate filters. *Proc. IMechE Part D: J. Automobile Eng.*, DOI: 10.1243/09544070JAUTO508.17.222:1471-1487.
- Arey J (2004). A tale of two diesels. *Environ. Health Perspect.*, DOI:10.1289/ehp.7031.112:812-813.
- Brown DM, Donaldson K, Borm PJ, Schins RP, Dehnhardt M (2003). Calcium and ROS-mediated activation of transcription factors and TNF- α cytokine gene expression in macrophages exposed to ultra-fine particles. *Am. J. Phys. Lung Cell Mol. Phys.*, <http://cat.inist.fr/?aModele=afficheN&cpsidt=15421220>,
- BS EN ISO 5167: Part 2: Measurement of fluid flow by means of pressure differential devices inserted in circular cross-section conduits running full. 286: 344-353.
- Dybdahl M, Risom L, Müller P, Autrup H, Wallin H (2003). DNA adduct formation and oxidative stress in colon and liver of big blue rats after dietary exposure to diesel particles. *Carcinogenesis*, DOI: 10.1093/carcin/bgg147.24:1759-1766.
- Gabathuler JP, Mizrah T, Eckert L, Fischer A, Kaser P, Maurer A (1991). "New Developments of Ceramic Foam as a Diesel Particulate Filter", SAE Paper no. 910325.
- Garshick E, Laden F, Hart JE, Rosner B, Smith TJ, Dockery DW, Speizer FE (2004). Lung cancer in railroad workers exposed to diesel exhaust. *Environ. Health Perspect.*, DOI: 10.1289/ehp.7195.112:1539-1543.
- Health Effects Institute, HEI, Perspectives, (2002) Understanding the health effects of components of the particulate matter mix: Progress and next steps. http://rds.yahoo.com/_ylt=A0geu4_NJOhJn9cAiadXNyoA;_ylu=X3oDMTE1dDhwNGY0BHNIYwNzcgRwb3Mheffects.org/Pubs/annualreport01-02.pdfDNwRjB2xvA2FjMgR2dGkA01BUDAwN18xMDY-/SIG=12bjfbsq/EXP=1240036941/**http%3a/www.health.
- Hinds WC (1980). "The drug and the Environment", *Sem. Medic. Respir.*, 1: 197-210.
- Macdonald IF, El-Sayed MS, Mow K, Dullien FAL (1979). "Flow through Porous Media – the Ergun Equation Revisited", *Industrial Engineering Chemistry Fundamentals*, 18: 198-208.
- Mayer A (1998). Selection Criteria for Diesel Particulate Trap Systems: VERT Experience. <http://www.dieselnet.com/papers/9812mayer.html>.
- Mayer A, Czerwinski J, Matter U, Wyser M, Scheidegger, Kieser D, Weidhofer (1998). "VERT: Diesel Nano-Particulate Emissions: Properties and Reduction Strategies", SAE No. 980539.
- Nauss K (1997). Diesel exhaust: A critical analysis of emissions, exposure and health effects. DieselNet technical report. <http://www.dieselnet.com/papers/9710nauss.html>.
- Nikula KJ, Finch GL, Westhouse RA, Seagrave J, Mauderly JL, Lawson DR, Gurevich M (1999). Progress in understanding the toxicity of gasoline and diesel engine exhaust emissions. Society of Automotive Engineers. Technical paper series. <http://www.osti.gov/bridge/servlets/purl/771098g01oIn/native/771098.pdf>.
- Pontikakis GN, Koltakis GC, Stamatelos AM (2001). Dynamic Filtration Modelling in Foam Filters for Diesel Exhaust, *Chemical Engineering Comm.*, 00: 1-26.
- Reader-Harris MJ, McNaught JM (2005). Best Practice Guide Impulse Lines for Differential-Pressure Flowmeters, NEL No.: 2005/224. http://rds.yahoo.com/_ylt=A0geu8g6H.hJYw4APNFXNyoA;_ylu=X3oDMTE2bWZ2MzcwBHNIYwNzcgRwb3MDMTEEY29sbwNhYz1EdnRpZANNQVAwMDdfMTA2/SIG=1442s42ps/EXP=1240035514/**http%3a/www.idconline.com/technical_references/pdfs/instrumentation/Differential%2520pressure%2520meters_nel.pdf.
- Richardson JT, Peng Y, Remue D (2000). "Properties of Ceramic Foam Catalyst Support: Pressure Drop", *Applied catalysis A: General* 204: 19-32.
- Siegmann K, Siegmann HC (1997). "The Formation of Carbon in Combustion and How to Quantify the Impact on Human Health, Euro physics news 28.
- Swiss Agency for the Environment, Forest and Landscape, SAEFL, 3003 Berne, (2000) Particulate Trap for Heavy Duty Vehicles, Environmental Documentation. No. 130. http://rds.yahoo.com/_ylt=A0geu7hnDehJywmANThXNyoA;_ylu=X3oDMTE1ZGw0b24zBHNIYwNzcgRwb3MDMQRjB2xvA2FjMgR2dGkA01BUDAwN18xMDY-/SIG=16oq3agei/EXP=1240030951/**http%3a/www.bafu.admin.ch/luft/00596/00597/00609/index.html%3flang=en%26download=NHZLpZig7t,lnp6i0NTU042i2Z6ln1ad1IZn4Z2zqZpnO2YUq2Z6gpJCDelB7fmym162dpYbUzd,Gpd6emK2Oz9aGodetmqnA19X12ldvoaCVZ,s-.pdf.
- Swiss Agency for the Environment, Forest and Landscape, SAEFL, 3003 Berne (2000) "Particulate Trap for Heavy Duty Vehicles", Environmental Documentation No. 130 http://www.umweltschweiz.ch/imperia/md/content/luft/fachgebiet/e/industrie/Partikelfilter_UM130_e.pdf for further details (last accessed 17th November 2004).
- United State Environmental Protection Agency, (2002) Health Assessment Document for Diesel Engine Exhaust. US Environmental Protection Agency, Office of Research and Development, National Center for Environmental Assessment, Washington Office, Washington, DC, EPA/600/8-90/057F. http://oaspub.epa.gov/eims/eimscomm.getfile?p_download_id=36319
- Warheit DB, Laurence BR, Reed KL, Roach DH, Reynolds GAM, Webb TR (2004). Comparative pulmonary toxicity assessment of single-wall carbon nanotubes in rats. *Toxicol. Sci.*, DOI: 10.1093/toxsci/kfg228.77:117-125.
- World Health Organization (2003). Health Aspects of Air Pollution with Particulate Matter, Ozone and Nitrogen Dioxide. Report on WHO Working Group, Bonn, Germany. EUR/03/5042688 http://rds.yahoo.com/_ylt=A0geu9SpCehJvQoAbRZXNyoA;_ylu=X3oDMTE1ZGw0b24zBHNIYwNzcgRwb3MDMQRjB2xvA2FjMgR2dGkA01BUDAwN18xMDY-/SIG=11v59svcc/EXP=1240029993/**http%3a/www.euro.who.int/document/e79097.pdf.